

heating of the compound nucleus followed by de-excitation by neutron emission only, overestimate the actual neutron yields by a factor of two or more if the commonly accepted interaction radius, $r_0 \approx 1.5 \times 10^{-13}$ cm, is used. However, refinements to the theory could change the predicted neutron yields by as much as the discrepancy between the experiments and the present theory. Before a more accurate comparison with the statistical model is possible, additional theoretical work and many more measurements, especially of the reaction

cross sections and the angle and energy distributions of the emitted neutrons, are necessary.

ACKNOWLEDGMENTS

We wish to thank C. M. Van Atta for encouraging this investigation, and Miss Margaret Thomas for numerical and other assistance. We also wish to thank Mr. Frank Grobelch for assistance in weighing foils, and the other members of the Hilac crew for assistance in performance during the experiments.

Nuclear Energy Levels of $\text{Na}^{24}\dagger^*$

CARL T. HIBDON

Argonne National Laboratory, Lemont, Illinois

(Received November 5, 1959)

The neutron cross section data up to 350 keV show a number of relatively large peaks and many smaller ones among the 86 peaks observed, the widths ranging from 0.2 to 6 keV. Approximately 50 small peaks were observed between 60 and 200 keV. Above 200 keV, each of the previously known peaks was resolved into two or more peaks and between these large peaks many narrower peaks were observed. The analyses show 9 *s*-wave levels and 46 *p*-wave levels, the remainder being *d*- and *f*-wave levels. A plot of the number of levels having energies $\leq E_n$ as a function of the neutron energy E_n shows an essentially linear distribution of the levels. As obtained from the reduced widths averaged over both values of J , the value of the strength function for $l=0$ is 0.06; averaged over all values of J for $l=1$ it is 0.65; and for higher values of l it is too large in comparison with the *p*-wave strength function.

I. INTRODUCTION

THE first measurements of virtual nuclear energy levels of Na^{24} in the keV region were made by Adair et al.¹ with a neutron energy spread of approximately 20 keV. They reported the presence of eight peaks in the region from 60 keV to 1 MeV. (All energies given in the present paper are neutron energies in the laboratory system.) Later Stelson and Preston² studied the region from 120 keV to 1 MeV with a neutron energy spread ranging between 2.5 and 5 keV and observed twelve resonances. One other resonance near 3 keV was also reported by Hibdon et al.³ Hibdon, Langsdorf, and Holland⁴ studied the region from about 2 to 80 keV with a neutron energy spread of 1.5 to 2 keV and confirmed the resonances near 3 and 55 keV. Several recent studies⁵ by different experimenters indicate that only

one resonance, near 3 keV, is present in the low-energy region.

The present paper is concerned with a study of the virtual nuclear energy levels of Na^{24} in the region from about 1 keV to 350 keV with the hope that the smaller neutron energy spreads currently in use⁶ could resolve other narrower resonances which may be present and not previously observed and that resonances already known could be better resolved. Since Na^{24} is an odd-odd nucleus and a close neighbor of the odd-odd nucleus Al^{28} , it might be expected to show a similar distribution in the level spacings, neutron widths and angular momenta (see Hibdon⁷ for Al^{28}). Both nuclei, being located near the predicted position of the giant resonance for the *p*-wave strength function, might also be expected to show a high value of the *p*-wave strength function. This expected high value was found⁷ for Al^{28} ; the present work also shows a high value for Na^{24} . The data on neutron cross sections are also

† Work performed under the auspices of the U. S. Atomic Energy Commission.

* The preliminary results of the measurements were reported at the meeting of the American Physical Society at Cleveland, Ohio, November 27-28, 1959 [Bull. Am. Phys. Soc. 4, 404 (1959)].

¹ R. K. Adair, H. H. Barschall, C. K. Bockelman, and O. Sala, Phys. Rev. 75, 1124 (1949).

² P. H. Stelson and W. M. Preston, Phys. Rev. 88, 1354 (1952).

³ C. T. Hibdon, C. O. Muehlhause, W. Selove, and W. Woolf, Phys. Rev. 77, 730 (1950).

⁴ C. T. Hibdon, A. Langsdorf, Jr., and R. E. Holland, Phys. Rev. 85, 595 (1952).

⁵ For a graphical display of the data obtained by the various experimenters and for references to the original papers, see

Neutron Cross Sections, compiled by D. J. Hughes and J. A. Harvey, Brookhaven National Laboratory Report BNL-325 (Superintendent of Documents, U. S. Government Printing Office, Washington, D. C., 1955), and Suppl. No. 1 (1957), and the 2nd ed., compiled by D. J. Hughes and R. Schwartz (1958). These compilations will be referred to as BNL-325. See also A. L. Toller, H. W. Newson, and E. Merzbacher, Phys. Rev. 99, 1625 (1955).

⁶ C. T. Hibdon, Phys. Rev. 108, 414 (1957).

⁷ C. T. Hibdon, Phys. Rev. 114, 179 (1959).

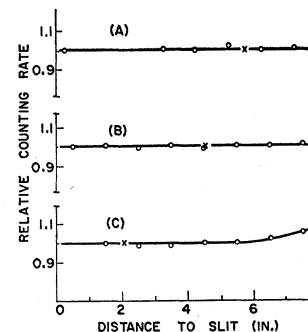
useful in reactor technology and for other practical applications.

2. EXPERIMENTAL METHOD

The experimental techniques and procedures are the same as were used previously and described in detail in the papers^{6,7} on Al²⁸ and on Fe and Cr. No further significant changes have been made in the basic counting equipment. However, the 90° electrostatic analyzer, which controls the energy of the Van de Graaff generator and selects the energy of the proton beam for high-resolution work, has been remounted. Precision compound cross slides have been installed to move the entrance and exit slits to align the analyzer⁸ and thereby avoid the loss of beam and change of voltage between the analyzer plates when the beam strikes the plates. The positions and widths of the slits are adjusted by micrometers. The entire assembly moves on ball bearings about a pivot point at the entrance slit and, when properly located, is locked in position. With the aid of some additional electronic equipment and grounded end blocks to indicate the position of the proton beam, just before and after the analyzer plates, the alignment of the analyzer now takes only a short time once the entrance slit is properly positioned. Considerable care was taken to level the analyzer and locate the proper positions of the slits. With this arrangement a proton beam current of 12 to 15 μ a could be maintained on the lithium target with no detectable current to the analyzer plates. A larger beam current was obtainable but was not used because the effects of so large a beam through the analyzer were not known, sufficient cooling for the slits and lithium target was not immediately available, and the speed of the necessary processing of the data could not be increased.

Samples of high-purity sodium metal of 2-in. diameter were sealed in aluminum cans having one-mil stainless steel end windows. The canning of the metal was done in a carefully dried box which had previously been evacuated for a long time and then filled with dry argon gas, thanks to L. S. Lackowicz of the Argonne Central Shops. The sodium was melted, poured into the cans, allowed to solidify, and then pressed to eliminate bubbles before sealing by use of O rings. When not in use the samples are stored in a desiccator. Previous experience has shown that samples prepared in this way can be kept for long periods. A series of samples ranging in thickness from 0.1 to 3 in. were prepared and are arranged in the wheels of a remotely-controlled sample changer so that any combination of samples up to 4.5 in. can be obtained in a few seconds. The effects of the end windows were undetectable. The background was found to be unaffected by the presence of the sample-changing wheels. This appears to be attributable

FIG. 1. Scattering-in of 75-kev neutrons by sodium samples and containers. Sample thickness: (A) 0.50 in., (B) 1.00 in., (C) 3.00 in. The crosses indicate the positions of the samples for neutron cross-section measurements.



to the small acceptance angle of the collimator of the neutron counter. The scattering-in effect of the sodium samples and their containers was also investigated for samples 0.5, 1.0, and 3.0 in. in length with neutrons at an energy of 75 kev. The relative counting rates corrected for background are shown in Fig. 1 for various positions of these samples. The points represented by crosses indicate the positions where the samples are placed for neutron cross-section measurements. Since these curves are horizontal straight lines (at least in the regions where the samples are normally used), no corrections for in-scattering are necessary. In the low-energy region the data show the 2.95-kev resonance of sodium but no resonance that might indicate the presence of impurities in the samples of sodium metal. A further check made by a spectrochemical analysis shows the presence of about 0.2% potassium. Other possible impurities were undetectable by this means of analysis.

The cross-section measurements were made from about 1 to 350 kev by use of neutrons whose energy spreads ranged between 350 and 400 ev, as given by the rise-curve method. A number of resonance were also studied by the self-detection technique.^{6,7} Briefly stated, flat-detection measurements are made when the scattering sample (see Fig. 1 of reference 6) in the neutron counter is made of a material (such as paraffin, Lucite, or graphite) that exhibits no resonance structure in the energy region of interest. Self-detection measurements are made when the transmission and scattering samples are of the same material. Thus the self-detection technique is a method which discriminates against neutrons whose energy differs much from that of the maximum of a resonance. The peak cross section determined thereby comes closer to the true peak height than does that determined by flat detection unless the width of the resonance is appreciably larger than the neutron energy spread. For these studies the scattering sample was sodium 300 mils thick, canned as described above. At higher energies it was necessary to use a scattering sample 500 mils thick in order to obtain a usable counting rate. A run with a similar empty can showed no appreciable effect so no correction was needed for the stainless steel end windows. The spread in energy of the neutrons was estimated by the

⁸ R. E. Holland, F. P. Mooring, and J. R. Wallace, Argonne National Laboratory Report ANL-5911, 1958 (unpublished), p. 2.

rise-curve method outlined in reference 6. Although no sufficiently narrow resonance at the higher energies is suitably isolated to study the spread in the energy of the neutrons, it is expected that the spread becomes somewhat larger at these energies.

3. EXPERIMENTAL RESULTS

The various figures show the observed neutron total cross section from about 1 to 350 keV. Unless otherwise stated the points obtained by flat detection are generally represented by open circles and the points obtained by self-detection are indicated by solid circles. The approximately 86 levels observed included all those found previously¹⁻⁴ and many new ones, the average level spacing being about 4.1 keV. Variations in the cross section show a more complicated level structure for Na^{24} than for the neighboring odd-odd nuclide⁷ Al^{28} . All of the large peaks observed by Stelson and Preston² were found to be composed of two or more peaks and between these large peaks many narrower peaks were observed. Only a relatively small number of peaks appear to be *s*-wave resonances ($l=0$) identifiable by their asymmetrical shapes and the presence of low minima on their low-energy sides. Because of the observable features of the data, one then expects a profusion of *p*- and *d*-wave resonances ($l=1, 2$, etc.) and the various peak heights seem to indicate the presence of an assortment of values for the angular momentum J . It can be seen by a casual examination of the data that the widths of the levels vary from about 0.20 keV to about 6 keV, compared with a range from 1 to 7 keV for Al^{28} .

It is especially interesting to know whether the levels of a single nucleus are distributed at random or at regular intervals. Whatever the manner of occurrence, a knowledge of the level spacings is of interest both for comparison with the theory of nuclear structure and for practical purposes such as the design of reactors. This is particularly true in the keV region because data in this region are less abundant than at low energies. It is also desirable to know whether a sizeable number of levels were missed during the measurements because of their very narrow widths. Figure 2 shows a plot of the number of levels at energies $\leq E_n$ as a function of the neutron energy E_n . This plot is essentially linear except at the lower energies. There is no downward curvature to indicate the general missing of levels in the high-energy region. The small variations from a straight line and the larger deviation at lower energies might indicate that a number of very narrow levels were missed. On the other hand, whatever model of the nucleus is appropriate, it is to be expected that the levels would be spaced somewhat at random. This random occurrence would then account for some of the deviations from linearity.

An examination of the data in the various figures shows a number of relatively large peaks scattered

among many smaller peaks, the peaks in the region from 60 to 200 keV being notable examples of the latter. Presumably the large and small peaks result from different types of interactions with the nucleus. According to the giant-resonance interpretation⁹ a truly single-particle interaction results in a large width of a level and hence in a reduced width approaching the Wigner limit $\hbar^2/\mu R^2$. When a number of nucleons in the nucleus are involved in the interaction, the reduced width of a level is expected to be much less than the Wigner limit. The reduced width is then expected to decrease as the number of nucleons involved in the interaction increases. The existence of many narrow levels would therefore be expected to be an indication of complex states.

The threshold of the reaction^{5,10} $\text{Na}^{23}(n,p)\text{Ne}^{23}$ is well above 4 MeV and therefore this reaction will not contribute to the cross section in the present measurements. The first excited state of Na^{23} appears to be at 440 keV and above this energy one might expect some inelastic scattering to begin. However, the inelastic neutron scattering cross section of Na^{23} has been measured in the region from about 440 keV to more than 800 keV by Hausmann et al.¹¹ They found peaks beginning at 482 keV. No peak has a cross section above 15 millibarns and it is noteworthy that their data do not show a well-defined peak in the region of the wide *s*-wave resonance found by Stelson and Preston² at 542 keV. The data do, however, show that a small wide peak may be present. From these measurements, one

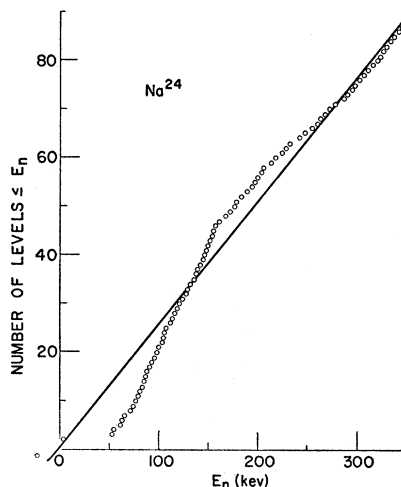


FIG. 2. Number of levels of Na^{24} with energies $\leq E_n$ as a function of the neutron energy E_n .

⁹ H. Feshbach, C. E. Porter, and V. F. Weisskopf, *Phys. Rev.* **90**, 166 (1953); A. M. Lane, R. G. Thomas, and E. P. Wigner, *Phys. Rev.* **98**, 693 (1955).

¹⁰ P. M. Endt and C. M. Braams, *Revs. Modern Phys.* **29**, 683 (1957).

¹¹ H. Hausman, J. E. Monahan, F. P. Mooring, and S. Raboy, *Bull. Am. Phys. Soc.* **1**, 56 (1956); J. E. Monahan, F. P. Mooring, and S. Raboy, Argonne National Laboratory Report ANL-5609, 1956 (unpublished), p. 106; and private communication.

concludes that the resonances of sodium, at least up to about 800 keV, may be treated as simple elastic scattering resonances, since the peak cross sections for inelastic and elastic scattering is approximately proportional to the corresponding widths ($\sigma_{\text{inel}}/\sigma_{\text{el}} \approx \Gamma_{\text{inel}}/\Gamma_{\text{el}}$) and the peaks of the resonances in question have total cross sections of several barns. Recently Bame and Cubitt¹² made measurements of the Na²³(*n*, γ)Na²⁴ process from about 20 keV to 1 MeV with large neutron energy spreads. Their data show broad maxima near 40, 110, 300, and 650 keV but no maximum exhibits a height above 3 mb so this cross section can also be ignored in the present analyses.

The various resonances at low energies may produce spurious peaks at higher energies because the neutron beam contains a second group of low-energy neutrons that arises from the formation of the residual nucleus Be⁷ in the 430-keV excited state.^{6,7} When the main group of neutrons has an energy of 284.4 keV, the low-energy component has an energy of 2.95 keV. Therefore, the 2.95-keV resonance reappears as a spurious peak at 284.4 keV, which thus (on the basis of relative peak heights) can be accounted for by assuming that about 0.6% of the beam of neutrons is in the low-energy group. Similarly, if at 357 keV the low-energy group constitutes about 5% of the beam, the small peak there may be a spurious reflection of the 54.1-keV resonance. Other small peaks up to 200 keV appear to be too small to reflect more than a few tenths of a barn at high energies.

4. ANALYSES OF THE RESONANCE LEVELS

A. Potential Scattering σ_p and the Number of Levels

Because of the observable features of the data, it does not appear that any of the 86 resonances, with the possible exception of the 2.95- and 54.1-keV resonances, can be analyzed as isolated levels. To obtain an analysis of any of the resonances one must first determine a value of the potential scattering σ_p that is reasonably close to its true value. In the past it has been customary to take for σ_p the lowest measured value of the cross section in a region which appeared to be relatively free of the wings of resonances. This procedure was used by Stelson and Preston² in their analyses of the levels of Na²⁴. They assumed a value of 3 barns for σ_p because this is the value indicated by their data below 200 keV and also in the region around 350 keV. However, they pointed out that this value for σ_p appeared to be too large and led to some inconsistencies that could not be readily explained. They also noted that the observed minimum of the *s*-wave resonance at 302.5 keV is below the theoretical minimum of $(1-g)\sigma_p$ [reference 7, Eq. (6)] for a value of $\sigma_p=3$ barns. Apparently their analyses were made on the assumption that the level spacing of Na²⁴ is sufficiently large that each level

could be treated as an isolated level so the interfering wings of other levels could be neglected. In the present data the many levels observed in Na²⁴ constitute a compelling argument against a value of σ_p as large as 3 barns. The overlapping and interfering wings of so many levels can be expected to contribute in every region a cross section quite significant in comparison with the true value of σ_p . The wings of *s*-wave resonances are known to extend relatively far from their peaks and, because of interference with the potential scattering, they may depress or elevate the cross section in a region which is otherwise well removed from resonances. This was shown to be the case⁷ for Al²⁸, so it should also be expected to happen in Na²⁴ which has a number of *s*-wave levels.

In the present measurements no region appears to be free of contributions from the wings of one or more resonances and this prevents a direct determination of σ_p from the data. The depths of the minima of the *s*-wave resonances indicate a value of σ_p lower than 3 barns. This is particularly true for the level at 302.5 keV, whose minimum is as well resolved as any other resonance. On the other hand the observed depth of this minimum is somewhat above the theoretical value of $(1-g)\sigma_p$ for $\sigma_p=1.9$ barns obtained from $\sigma_p = \sum_l (2l+1)4\pi\lambda^2 \sin^2\delta_l$. The data do show a number of neighboring resonances whose wings certainly contribute to the cross section in the region of this minimum. Also the wide *s*-wave resonance at 542 keV is known to mutually interfere with the level at 302.5 keV and can be expected to add a small amount at its minimum. Consequently, the true single-level depth of the minimum of the resonance at 302.5 keV can not be determined directly from the data. In view of the foregoing observations it appears that the true value of the potential scattering may be expected to be close to the theoretical value $\sigma_p = \sum_l (2l+1)4\pi\lambda^2 \sin^2\delta_l$. This value of σ_p differs but little from the value of 2.4 barns obtained by Lynn et al.¹³ in a study of the 2.95-keV resonance. Therefore, the theoretical value of σ_p will be assumed for the present analyses and the consequences compared with the data.

The method of analysis⁷ is essentially the same as that used for Al²⁸. By use of estimated parameters, single-level plots are made until a best fit to the data is obtained. If necessary, multiple-level plots are included and the parameters adjusted to obtain a still better fit. The analyses proceed more directly if the *s*-wave levels are first located and their multiple-level plots subtracted from the data to remove σ_p and the extensive interfering wings of these levels. One then continues the analyses by considering first the more prominent resonances whose wings are best exposed. For some groups of resonances this was not practical because of multiple subtractions. In these cases it was necessary to estimate the parameters and compare the multiple-level plots

¹² S. J. Bame and R. L. Cubitt, Phys. Rev. **113**, 256 (1959).

¹³ J. E. Lynn, F. W. K. Firk, and M. C. Moxon, Nuclear Phys. **5**, 603 (1958).

with the data and adjust the parameters until a best fit was obtained. The equations used for these analyses are Eqs. (1) to (6) of reference 7. Programs for the many tedious calculations needed in these analyses have been set up for machine computation by the Applied Mathematics Division. One program for the IBM-704 is used to calculate points over the resonances and the needed portions of the wings by use of the Breit-Wigner multiple-level dispersion formula. The program includes the variation of the widths of the levels with energy in accordance with $\Gamma_n = 2P\gamma^2$, where $P_0 = x$, $P_1 = x^2/(1+x^2)$, etc., with $x = R/\lambda$. The nuclear radius was assumed to be $1.4A^{1/3} \times 10^{-13}$ cm.

A program has also been set up for the computer GEORGE to determine the location and width of a resonance by the method of least squares. It is useful for resonances whose wings are relatively free from interference with other resonances and for which a reasonably close initial estimate of the parameters can be made. This program can also determine simultaneously the parameters of two mutually interfering resonances. It also includes the variation of the width of a level with energy, $\Gamma_n = 2P\gamma^2$. The parameters found are then used to obtain plots by use of the IBM-704 computer. The plots for every resonance were compared with the data and the parameters were adjusted until a reasonable fit was obtained.

It is to be noted that the levels of Na^{24} are narrower than those of Al^{28} and, therefore, the determination of the total angular momentum J is usually more difficult.

Sodium has only one stable isotope, Na^{23} ; so all observed resonances are levels of the compound nucleus Na^{24} . The nuclear spin⁹ of Na^{23} is $I = \frac{3}{2}$ and the parity of the ground state is even. Then the levels of the compound nucleus formed by s -wave neutron interaction ($l=0$) have a possible J of 1 or 2 and even parity; those formed by p -wave neutrons ($l=1$) have a possible J of 0, 1, 2, or 3 and odd parity; and those formed by d -wave neutrons ($l=2$) a possible value of J of 0, 1, 2, 3, or 4 and even parity. For f -wave neutrons ($l=3$) the possible values of J are 1, 2, 3, 4, and 5 and the parity is odd. Hence the possible combinations of J and parity for $l \leq 3$ may lead to any of 11 types of resonances for the compound nucleus Na^{24} .

B. Analysis of the 2.95-Kev Resonance

During the present experiments the 2.95-kev resonance was studied intensively both by flat- and by self-detection techniques.⁶ A graphite scattering sample 6 in. thick was used for the flat-detection and a sodium scattering sample 300 mils thick for the self-detection measurements. The data, Fig. 3, show the wings of this resonance to be very definitely asymmetrical in shape with comparatively high values of the cross section on the high-energy side. This asymmetry appears to be sufficient to establish an s -wave neutron

interaction ($l=0$) for this resonance despite the fact that the minimum on the low-energy side is broad and less pronounced than is usually observed with an isolated level of this type. Self-detection data are shown in the insert of Fig. 3 from which it may be seen that the width at half the measured height is about 300 ev. Since the resonance does not appear to be fully resolved to its true height, the actual width would then be expected to be somewhat less than 300 ev.

Because of its unusual shape and its importance in reactor technology, various experimenters have studied this resonance, but its shape, its narrow width and its high peak cross section have prevented an unambiguous determination of its parameters. Results of initial experiments⁸ were interpreted to give a value of $J=2$ and $l=0$ but recently Lynn, Firk, and Moxon¹³ interpreted their data to show a value of $J=1$ with a preference for $l=0$. Good, Neiler, and Gibbons¹⁴ interpreted their data in a similar way. Block¹⁵ measured the angular distribution of the neutrons in the region of this resonance and his results strongly favor a value of $l=0$. Some experimenters² have suggested that this resonance might be formed by a p -wave neutron interaction, but others^{13,15} pointed out that the reduced width would then be much greater than the Wigner upper limit on reduced neutron widths.

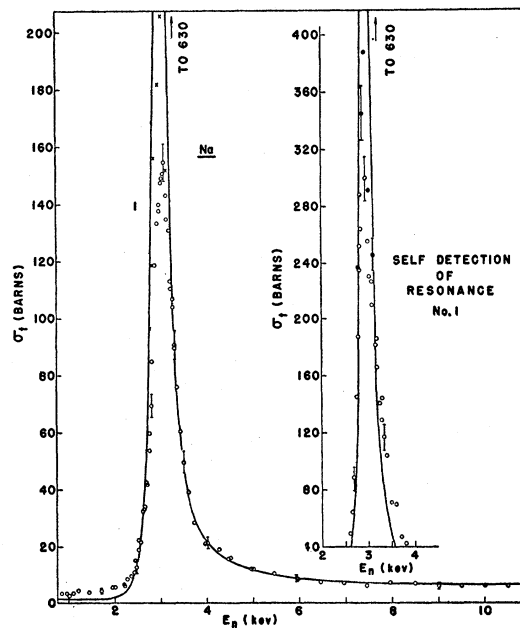


FIG. 3. Neutron total cross section of sodium up to 10.5 kev. Crosses show data obtained with a neutron energy spread of about 300 ev and the open circles the data for a neutron energy spread of about 400 ev. The insert shows the results obtained by self-detection for the same neutron energy spreads. The curve shows the theoretical plot obtained by a multiple-level computation of all s -wave levels ($J=2$) including a bound level at -30 kev.

¹⁴ W. M. Good, J. H. Neiler, and J. H. Gibbons, Phys. Rev. **109**, 926 (1958).

¹⁵ R. C. Block, Phys. Rev. **109**, 1217 (1958).

Possible values of the peak heights of this resonance for $l=0$ are about 370 and 630 barns corresponding to values of $J=1$ and 2, respectively. In view of these high peak values and a width as narrow as 200 to 300 ev, it would appear that neutron energy spreads currently in use are really too large to resolve this resonance sufficiently to clearly distinguish between the two possible values of J and one then must resort to some other means to find the value of J . It is doubtful that one can reach a peak height comparable to that for $J=2$ by use of current neutron energy spreads.

Because the peak height which can be attained in the present experiments will depend on the thickness of the sodium transmission sample and on the neutron energy spread, lithium targets of different thicknesses were used to gain information concerning the relative peak heights to be expected from the various measurements. In the present experiments the over-all neutron energy spread appears to be about one-half the thickness of the lithium target indicated by the rise-curve method.⁶ The results of these studies are shown in Fig. 4. Curves A and C indicate the relative peak heights to be expected for a sodium sample 100 mils thick measured by flat detection and by self-detection, respectively. The point shown by a solid circle on curve A was obtained during a previous experiment. A second point by a solid circle above it was obtained by use of a sample of sodium 50 mils thick. For comparison the two points shown by a cross and a triangle indicate, respectively, the corresponding peak heights attained at Harwell¹³ and Oak Ridge.¹⁴ The measurements at Harwell were made with a neutron energy spread of about 150 ev and a sample of sodium about 60 mils thick, while those at Oak Ridge were made with an energy spread of about 200 ev and a sample approximately 20 mils thick. Curve B, then, indicates the approximate peak height to be expected for a sample of sodium 50 mils thick.

The general trend of these curves in Fig. 4 shows that

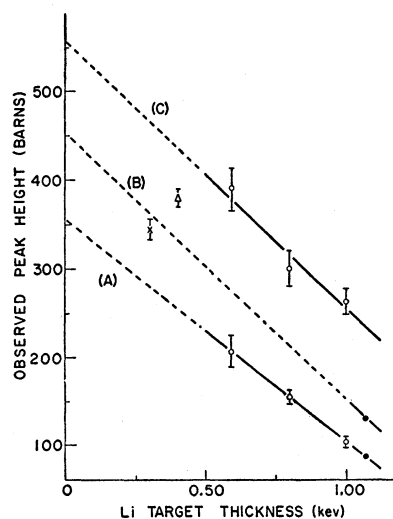


FIG. 4. Observed peak height of the 2.95-keV resonance of sodium as a function of the thickness of the lithium target. The target thickness is approximately double the neutron energy spread. See text for explanations.

one can expect progressively higher peak values of the resonance as decreasing neutron energy spreads and thinner sodium samples are used and that the expected peak values are within reasonable limits. Projections of the curves to the region of small neutron energy spreads indicate that the true peak height of the 2.95-keV resonance is well above 500 barns. By self-detection and a sample of sodium about 25 mils thick one could expect to attain a peak height of about 600 barns if a neutron energy spread of about 50 ev could be used. One then concludes that the correct value of J is 2 since the corresponding theoretical peak height is about 630 barns.

No set of parameters for a single-level plot has been found that will provide a perfect fit for both wings of the 2.95-keV resonance for values of $l=0$ or 1. The similarity in the shapes of the peaks and wings of the 2.95-keV resonance in Na²⁴ and the 35-keV resonance already analyzed⁶ in Al²⁸ suggests that one can expect strong mutual interference to be associated with the resonance in sodium. The cross section in the high-energy wing of the sodium resonance is so high and the wing so extensive that only a strong mutual interference with a bound level can be expected to account for it. No other level has been observed in the immediate region of the 2.95-keV resonance. Therefore, any strong mutual interference must be attributed to a bound level. Apparently the bound levels of Na²⁴ have not been studied¹⁰ above 4.7 Mev and one must then deduce the location of the bound level and its reduced width from the present data. Lynn, Firk, and Moxon¹³ attempted to fit their data on the 2.95-keV resonance ($J=1$, $l=0$, and $\Gamma_r=405$ ev) by including the contributions of a bound level ($J=2$, $l=0$) but the calculated curve does not fit their data below 800 ev nor above 5 keV.

Many calculations have been made during the present analyses in an attempt to fit this resonance by including the mutual interference with a bound level. Values of E_r from -1 to -60 keV have been assumed with various values for the reduced width γ^2 . Not even the least-squares computations by the computer GEORGE have found a combination of parameters for the resonance and the bound level that duplicates the observed data everywhere. This is apparently attributable to the high value of the cross section in the low-energy wing of resonance No. 1. This method does, however, always indicate a width of about 0.22 keV and a location near 2.95 keV for resonance No. 1 but fails to provide reasonable parameters for the bound level. The high-energy wing can be fitted fairly well even far away from the resonance. The calculated cross section then fits the low-energy wing near the resonance but deviates from it away from the peak. However, all of these calculations show values of $E_r=2.95$ keV, $\Gamma_r=0.22$ keV, $J=2$, and $l=0$.

Many sets of provisional parameters were tried and it was found that a best fit occurs if the bound level

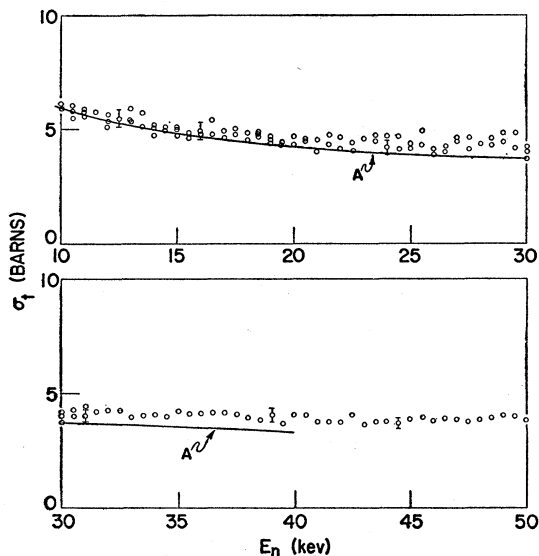


FIG. 5. Neutron total cross section of sodium from 10 to 50 keV.

is assumed to be located at -30 keV and its reduced width is $\gamma^2=30$ keV. This plot very closely duplicates the shape of the high-energy wing up to about 35 keV, but begins to drop below the data in the low-energy wing below about 2.4 keV. This drop in the low-energy wing occurs for any set of parameters that provides a fit for the high-energy wing. This would then indicate that the high-energy wings of other bound levels may extend into this region and account for the extra cross section needed in the region up to 2.4 keV. However, the wings of these peaks can not be included in the present calculations until their locations are known.

If a p -wave neutron interaction is assumed for the two levels, the closest fit to the data occurs for a bound level at -4 keV with a reduced width of 2000 keV along with a reduced width of 1400 keV for the 2.95-keV resonance. However, the fit to the data in the low-energy wing of the 2.95-keV resonance is very little better than for $l=0$. The region around 3.5 to 5 keV does not appear to be fitted by any set of parameters for a p -wave neutron interaction.

The solid curves in Figs. 3 and 5 were obtained by use of the parameters shown in Table I and represent the best fit obtained. All resonances having $l=0$ and $J=2$ were included in the multiple-level computation.

The region between 10 and 50 keV shown in Fig. 5 is the largest one which is free of prominent levels and one might at first expect to find the observed cross section here to be approximately equal to the potential scattering cross section. However, throughout this region the cross section is consistently well above the expected potential scattering. This high average value of the cross section may be attributed to the extensive wings of resonances which extend into this region, to the presence of a number of very narrow levels in this region, or to a combination of both. In the analysis of

the 2.95-keV resonance, the high-energy wing was computed up to 40 keV in this region and is shown by curve A in Fig. 5. This curve was obtained by a multiple-level calculation for all of the s -wave levels to which a value of $J=2$ was assigned and appears to account for the general trend of the data. The wings of a number of bound levels may extend into this region and their contributions may be sufficient to fully account for the behavior of the cross section in this region. On the other hand, the variations of the cross section in Fig. 5 indicate that a number of unresolved levels may be present. An attempt was made to investigate a number of these possible peaks by self-detection but the data obtained did not improve on those in Fig. 5.

C. Analysis of the 54.1- and 55-KeV Resonances

The resonance which appears to be located at 54.2 keV was also studied in detail by use of a lithium target 0.8 keV thick (as determined by the rise-curve method) and a sample of sodium 100 mils thick. It was resolved to a height of 26.5 barns by flat detection and 37 barns by self-detection.⁶ A graphite scattering sample 6 in. long was used for flat detection and a scattering sample of sodium 300 mils thick for the self-detection measurements. During later measurements a further study of this resonance was made by use of a lithium target

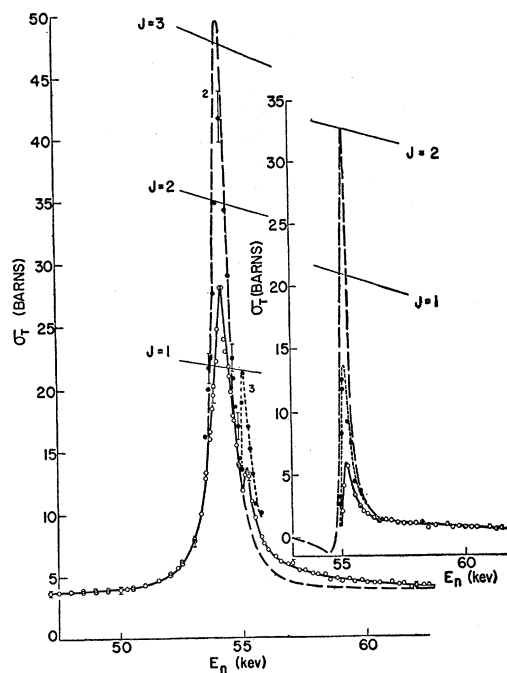


FIG. 6. The 54.1- and 55-keV resonances of Na^{24} . Points represented by open circles were obtained by flat detection and those represented by solid circles by self-detection. The dashed curve shows the single-level plot obtained by parameters discussed in the text. The insert shows the 55-keV resonance after subtracting the single-level plot of resonance No. 2 from the data. The dashed curve in the insert shows a multiple-level plot for the s -wave levels having a value of $J=2$. The loci of the theoretical single-level peak heights are also shown.

TABLE I. Summary of the levels of Na²⁴ derived from neutron reactions with Na²³. The parameters J , Γ , and l are probable values obtained as a best fit to the data.

No.	E_r (kev)	J	Γ_n (kev)	l	No.	E_r (kev)	J	Γ_n (kev)	l
1	-30.0	2		0	31	154.9	1	0.45	2
	2.95	2	0.22	0	32	156.6	1	0.45	2
2	54.1	3	0.75	1	33	160.8	0	2.00	1
3	55.0	2	0.20	0	34	167.3	0	1.7	1
3A	61.5	0	0.30	1	35	171.8	0	2.2	1
4	63.6	1	0.40	1	36	175.7	0	1.9	1
5	66.8	1	0.40	1	37	178.4	0	1.7	1
6	72.5	2	0.30	1	38	182.6	0	2.0	1
7	75.7	0	0.55	1	39	188.0	1	1.6	1
7A	77.6	0	0.50	1	40	193.0	1	1.2	2(1)
8	79.9	0	0.60	1	41	196.7	1	1.1	2(1)
9	81.5	0	0.70	1	41A	199.5	2	0.7	2
10	83.9	0	0.65	1	42	202.7	3	1.8	1
11	85.3	0	0.35	1	43	205.2	1	3.6	0
11A	86.4	0	0.30	1	44	213.7	2	1.3	1(2)
11B	88.4	0	0.40	1	45	218.2	2	1.2	1(2)
11C	91.3	1	0.45	1	46	224.0	1	1.7	1(2)
12	93.0	1	0.50	0	47	227.7	1	1.7	1(2)
13	96.5	0	1.00	1	48	231.9	2	0.9	0
13A	98.6	1	0.45	1	49	242.0	2	6.0	1
13B	100.9	1	0.35	1	50	246.3	1	3.0	0
13C	103.2	0	0.50	1	51	255.0	2	1.3	2
13D	104.3	0	0.55	1	52	260.5	1	1.7	2(1)
13E	105.9	1	0.35	1	53	264.7	1	0.9	2
14	107.4	1	0.45	0	54	268.5	2	1.1	2
15	111.5	1	0.55	1	55	272.8	1	1.1	2
15A	113.5	0	0.60	1	56	278.5	1	1.3	2
15B	116.7	1	0.50	1	57	287.0	1	1.3	2
15C	118.4	1	0.60	1	58	290.7	2	0.9	2
16	120.2	1	0.50	0	59	294.7	1	1.3	2
17	124.0	0	0.90	1	59A	298.0	0	2.0	2
18	127.2	1	0.50	1	60	302.5	2	2.5	0
19	129.2	0	0.70	1	61	306.5	0	1.6	2
20	131.8	0	1.00	1	62	311.8	1	1.5	2
21	134.9	1	0.70	1	63	316.5	2	0.9	3(2)
22	137.5	1	0.40	2	63A	321.0	1	0.9	3(2)
23	138.9	1	0.40	2	64	324.0	1	1.3	2
24	141.5	1	0.70	1	64A	326.8	1	0.9	3(2)
25	144.2	1	0.50	2	65	330.8	1	2.0	2
26	146.0	1	0.50	2	65A	334.2	1	1.0	3(2)
27	147.6	0	0.40	1	66	338.3	1	1.7	2
28	149.3	0	0.75	1	67	343.6	2	1.0	3(2)
29	150.7	0	0.80	1	67A	346.0	1	0.75	3(2)
30	153.2	1	0.40	2					

approximately 0.7 kev thick. The peak was resolved to a height of 28 barns by flat detection and 43.5 ± 3.5 barns by self-detection. These results indicate a value of $J=3$, the corresponding single-level peak height being about 47.5 barns for this value and about 35 barns for $J=2$. A plot of the data is shown in Fig. 6. Because of its apparent symmetrical shape with no discernible interference dip on its low-energy side, this resonance is taken to be formed by a p -wave neutron interaction. Measurements of the differential elastic neutron scattering cross section in this region by Block, Haeberli, and Newson,¹⁶ although somewhat inconclusive, also indicate a p -wave neutron interaction.

This resonance appears to be sufficiently removed from other interfering resonances to permit treating it as a single level. It does, however, sit on an apparent background of 3.6 barns. A best fit for a single-level plot occurs when the parameters shown in Table I are

¹⁶ R. C. Block, W. Haeberli, and H. W. Newson, Phys. Rev. 109, 1620 (1958).

used, but a complete fit for the high-energy wing is not obtainable with any set of parameters because of the presence of the small peak at 55 kev. This small peak has been thoroughly investigated by flat detection and by self-detection. Flat-detection measurements always showed a small peak in the high-energy wing of the 54.1-kev resonance. The peak is much more pronounced when self-detection measurements are made.

By subtracting the single-level plot of the 54.1-kev resonance from the data, one finds that the peak near 55 kev is left with a peak height (self-detection) of about 12.5 barns compared with possible heights of 4.8, 17.8, and 29 barns (exclusive of potential scattering) for $J=0, 1, \text{ and } 2$, respectively, and must therefore, have a value of $J \geq 1$. A plot of these results, shown as an insert in Fig. 6, indicates a width of 300 ev or less. Its width is less than the neutron energy spread and neither method of detection will resolve it sufficiently to determine the value of J directly from its peak height alone. However, its shape (especially its high-

energy wing) is so characteristic of an s -wave neutron interaction that no other assignment appears to be possible, although certainly some inaccuracies are to be expected in the subtractions. The level is obviously so narrow that one can not determine its width directly. However, the high-energy wing above about 56.5 keV appears to be fairly well established and the parameters of this resonance would then be expected to account for this wing.

Single-level plots for widths ranging from 200 to 300 eV and for both $J=1$ and 2 were made in attempting to determine the parameters of the 55-keV resonance. Finally, it was found that a multiple-level plot of all the s -wave levels ($J=2$) gave the best fit when the parameters shown in Table I are used. For $J=1$ the computed points in the high-energy wing always fell below the corresponding points shown in the insert of Fig. 6. A width of 0.20 keV for this level provides a best fit for the data when the cumulative mutual interference of all s -wave levels ($J=2$) is included.

The minimum of resonance No. 3 then depresses the peak of No. 2 by more than a barn, depresses its low-energy wing, and elevates its high-energy wing. The result is to shift the peak near 54 keV to a position slightly above the true energy of the resonance. By making the correction for the low-energy wing of the 55-keV resonance, the true location was found to be at 54.1 keV and that of No. 3 at 55.0 keV. A re-subtraction of the high-energy wing of the 54.1-keV resonance from the data then shows a slightly larger width and a slightly higher peak for the 55-keV resonance. The plot in the insert of Fig. 6 shows the corrected data. If the corrections are omitted, the two resonances appear to be located at 54.2 and 55.1 keV.

D. Analysis of the Resonance Levels from 60 to 180 KeV

In this region, many small peaks of various heights and generally narrow widths were observed. From about 60 to 100 keV, repeated measurements with flat detection (even by the smallest usable neutron energy spreads) failed to resolve a number of the peaks well enough to determine their J values directly from the observed peak heights. To reach higher values near the peaks of these levels, measurements were made over the entire region by self-detection at 0.5-keV intervals. The results of the various measurements are shown in Figs. 7, 9, 11, and 13 in which open circles are used to represent data obtained by flat detection and solid circles the data obtained by self-detection. Even by self-detection, many of the peaks do not appear to be resolved to heights that are close to their true heights. The peaks are narrow, the wings are steep, and the distribution of the neutron energies does not break off sharply at the edges. It is, therefore, recognized at the outset that the values of J determined for some of these peaks may only be minimum values and hence

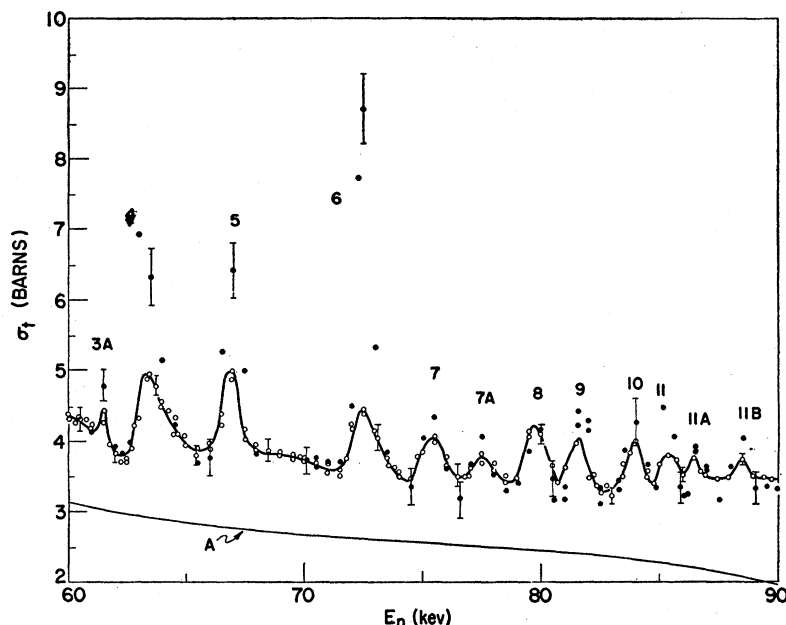
that the corresponding widths would be wider than the true widths.

The measurements of neutron-capture cross section by Bame and Cubitt¹² revealed a broad resonance near 115 keV. It can be shown by use of the Breit-Wigner single-level dispersion formula that when neutron capture is not negligible, the peak height of a resonance is reduced below the elastic-scattering height by the factor Γ_n/Γ , where Γ_n is the neutron elastic-scattering width and Γ the total width of a resonance. However, the factor Γ_n/Γ is not known for any particular one of these levels; nor is an average value known for a group of levels because the distribution of the capture cross section among the various levels is not known. There appears to be no way at present to identify the levels with which the capture cross section is associated nor to determine the factor Γ_n/Γ for them. However, because of the low peak height of 1.5 millibarns for the absorption resonance at 115 keV and its large width, one would not expect the factor Γ_n/Γ to differ very much from unity for any resonance in this group.

The average total cross section is fairly high in this region, which in itself is an indication of considerable level structure. The many observed levels and their overlapping and interfering wings are the principal contributors to this high average cross section because no wide levels occur in or near this region and the wings of s -wave levels in other regions are known to make relatively small contributions in this region. At a first glance, the low observed peak heights of these levels might be taken to indicate a trend toward low values of J in this region. Undoubtedly this is true for many of the peaks because their widths are sufficient to establish a value of $J=0$. For a number of levels, however, the heights of the peaks are sufficient to rule out a value of $J=0$ but insufficient to make a clear distinction between $J=1$ and 2.

There are a number of observable features in the data that aid in identifying these levels: (a) A comparison of the relative peak heights of a number of the resonances with the height of No. 3 (Fig. 6) indicates that a value of $J=1$ or 2 is appropriate for a considerable number of these levels. (b) The presence of deep minima between various pairs of adjacent peaks indicates mutual interference but the absence of deep minima between other pairs suggests that either J or l must differ for the pair unless unresolved levels are filling in the valley between the peaks. (c) Discernible dips, characteristic of s -wave resonances, are present on the low-energy sides of a few of these peaks and this limits the value of J for these levels to 1 or 2. A comparison of the relative widths and peak heights of nearby p -wave levels with the s -wave levels then serves to indicate the value of J for the p -wave levels. (d) The reduced widths obtained from neutron widths that appear to account for these levels are very near or exceed the Wigner limit on d -wave interactions for

FIG. 7. Neutron total cross section of sodium from 60 to 90 kev. Open circles show data obtained by flat detection; solid circles data by self-detection. Curve *A* is a multiple-level plot of the *s*-wave levels that extend into this region.



most of these levels. They must, therefore, be *p*-wave levels.

Consider first the region from 60 to 90 kev, which is shown in Fig. 7. Apparently no *s*-wave levels are present in this small region, since there are no clearly defined dips on the low-energy sides of the peaks and the peaks are not asymmetrical in shape. Moreover, the high average value of the cross section below about 63 kev is hardly explicable in the presence of *s*-wave levels in this region, because the low-energy wings of any such peaks would interfere with the potential scattering and reduce the average cross section below the observed value. The wings of various *s*-wave resonances in other regions do, however, extend into this region and their combined contribution plus the potential scattering cross section is shown by curve *A* in Fig. 7. This curve also includes the low-energy wings of the *s*-wave resonances Nos. 12, 14, and 16 (see Figs. 9 and 11). By subtracting curve *A* from the data in Fig. 7, one obtains the curve shown in Fig. 8. This curve represents the cross section produced by the resonances and their overlapping and interfering wings. Because of the relative peak heights and widths of these resonances, one expects (a) a value of $J=0$ for peak No. 3A and for the group Nos. 7 through 11B, (b) $J \geq 1$ for Nos. 4 and 5, and (c) $J \geq 2$ for No. 6. Because of their apparent widths, all of these peaks are expected to be attributable to *p*-wave neutron interactions, and mutual interference among various levels having common values of J is expected. The minima between pairs of adjacent levels in the group Nos. 7 through 11B, considered with the level spacings, are compatible with the expected mutual interference. One or more of the peaks in the group Nos. 7 through 11B might be expected to have a value of J of at least 1, but,

on the basis of the present data, one is compelled to assume a value of $J=0$ for each resonance in this group. Although some of these peaks are relatively narrow, they are wide enough to indicate that fully resolving them would be expected to give peak heights corresponding to the theoretical values for $J=0$. A multiple-level plot was made for the group of peaks Nos. 7 through 11B; it is shown as a dashed curve in Fig. 8. According to this curve, the widths of these peaks can be no greater than the widths listed in Table I. If it can be shown that the true peak heights of some of these levels are much higher and the correct value of J is 1 rather than 0, then correspondingly narrower widths would account for the data.

The peak heights of Nos. 4 and 5 compared with Nos. 7 through 11B would then certainly indicate a

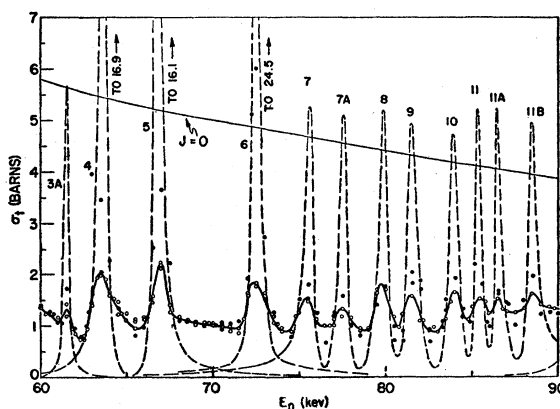


FIG. 8. Analyses of the level of Na²⁴ from 60 to 90 kev. The points shown were obtained by subtracting curve *A* in Fig. 7 from the data. The dashed curves are the theoretical plots obtained by use of the resonance parameters listed in Table I.

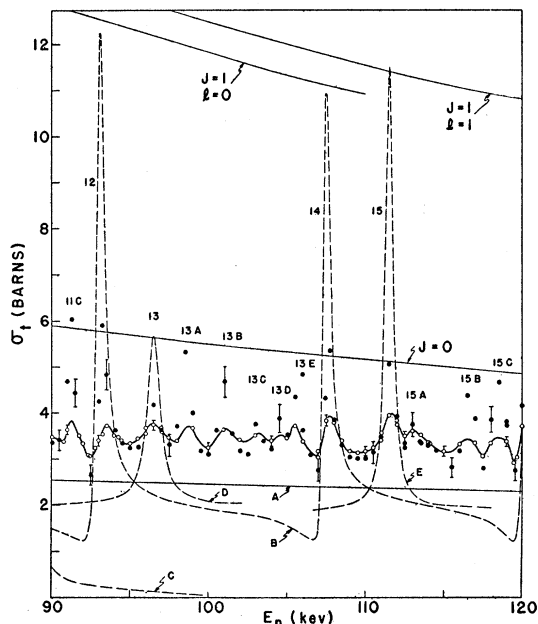


FIG. 9. Neutron total cross section of sodium from 90 to 120 keV. Open circles show data obtained by flat detection; solid circles data by self-detection. Curve *A* is a multiple-level plot of the *s*-wave levels that extend into this region; curve *B* is a multiple-level plot of the *s*-wave levels Nos. 12, 14, and 16 and curves *D* and *E* are single-level plots of the *p*-wave levels Nos. 13 and 15. Curve *C* is a continuation of the multiple-level plot in Fig. 8.

minimum value of $J=1$ for the former two resonances. There should, then, be mutual interference between these two peaks. In this event one expects to see a lower minimum between them, but the irregularities in the cross section between these two peaks and the shape of the high-energy wing of No. 4 provide some indication of the presence of other levels too narrow to be resolved. The parameters listed in Table I were used to obtain the multiple-level plot for these two levels (shown by a dashed curve in Fig. 8). Since resonance No. 6 has the highest observed peak height in this region, it is expected to have $J \geq 2$. A single-level plot is shown in Fig. 8 for this resonance. A single-level plot is also shown for the small peak No. 3*A* for a value of $J=0$ and $\Gamma_n=0.30$ keV.

Figure 9 shows the data from 90 to 120 keV. Because of the dips on the low-energy sides of peaks Nos. 12 and 14, these two peaks are taken to be narrow *s*-wave levels. The presence of peak No. 11*C* so near the minimum of No. 12 and No. 13*E* so near the minimum of No. 14 prevents one from observing lower minima on the low-energy sides of Nos. 12 and 14. Their observed peak heights are relatively low so the value of J is taken to be 1 for each level. The multiple-level plot of these two resonances together with No. 16 (Fig. 11) for the parameters listed in Table I is also shown as curve *B* in Fig. 9. Single-level plots for No. 13 ($J=0, l=1$) and No. 15 ($J=1, l=1$) are also shown

as curves *D* and *E*, respectively. Curve *A* shows the potential scattering plus the combined contributions of *s*-wave levels in other regions. Curve *C* is a continuation of the multiple-level plot in Fig. 8. When curve *A*, curve *C*, and the resonance contributions of Nos. 12, 13, 14, and 15 are subtracted from the data, one obtains the curves shown in Fig. 10. These curves show only the resonance contributions of the remaining peaks in this region.

The observed peak height of No. 11*C* in Fig. 10 is only slightly above the theoretical height for $J=0$, but a resonance as narrow as this can be expected to be resolved to a much greater height by a smaller neutron energy spread. Therefore, the value of J is taken to be 1. The single-level plot for a width of 0.45 keV and $l=1$ (shown dashed in Fig. 10) represents the greatest width this level can have for a value of $J=1$.

Taking into account the relative peak heights, apparent widths, and overlapping wings of the group of peaks Nos. 13*A* through 13*E*, one expects a value of $J=1$ for Nos. 13*A*, 13*B* and 13*E* and $J=0$ for Nos. 13*C* and 13*D*. Mutual interference will then occur for the three resonances having a value of $J=1$ and also for the two having the value of $J=0$. These two multiple-level plots, shown in Fig. 10 for the widths tabulated in Table I, appear to be in accord with the data except near the peaks.

Because of the relative peak heights and apparent widths, the value of J is taken to be 0 for No. 15*A* and 1 for Nos. 15*B* and 15*C*. With an apparent width as large as that of 15*A*, smaller neutron energy spreads would not be expected to resolve the peak to a height corresponding to $J=1$. A single-level plot for $\Gamma_n=0.60$ keV for No. 15*A* and a multiple-level plot for Nos. 15*B*

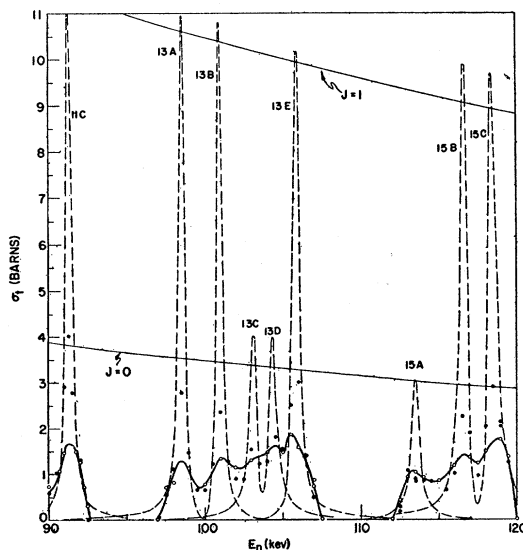


FIG. 10. Analyses of the levels of Na^{24} from 90 to 120 keV. The points shown were obtained by subtracting curves *A* to *C* inclusive from the data in Fig. 9. The dashed curves show the theoretical plots obtained by the resonance parameters in Table I.

and 15C for widths of 0.50 and 0.60 keV, respectively, are shown in Fig. 10. The spacing between Nos. 15B and 15C appears to be too small for observation of a minimum as deep as the theoretical minimum.

The data from 120 to 150 keV are shown in Fig. 11. Peak No. 16 exhibits a dip in the cross-section data on its low-energy side and an apparently asymmetrical shape. It is, therefore, taken to be an *s*-wave level. Because of the relatively low observed peak, a value of $J=1$ is assumed. The proximity of peak No. 15C to the minimum of No. 16 prevents one from observing a deeper minimum on the low-energy side of No. 16. Curve B in Fig. 11 is a continuation of the multiple-level plot of peaks Nos. 12, 14, and 16 from Fig. 9. It includes the potential scattering. Curve A also includes the potential scattering and shows a multiple-level plot of the *s*-wave levels in other regions. Curve C is a continuation of the multiple-level plot of Nos. 15B and 15C in Fig. 10. When curve A and the resonance contribution of curve B are subtracted from the data, one obtains the solid curve shown in Fig. 12. This curve is then the resonance contribution of the remaining levels in this region.

Because of the relative peak heights and apparent widths of the levels shown in Fig. 12, the value of J is expected to be 0 for peaks Nos. 17, 19, and 20 and 1 for each of the remaining peaks in Fig. 12, with the exception of No. 27. At a first glance Nos. 17, 19, and 20 might appear to have a small width and therefore to be associated with a higher value of J ; but a comparison with the peak heights of Nos. 22, 23, 25, and 26, levels of similar apparent widths, disfavors a value of $J=1$ for Nos. 17, 19, and 20. The multiple-level plot for Nos.

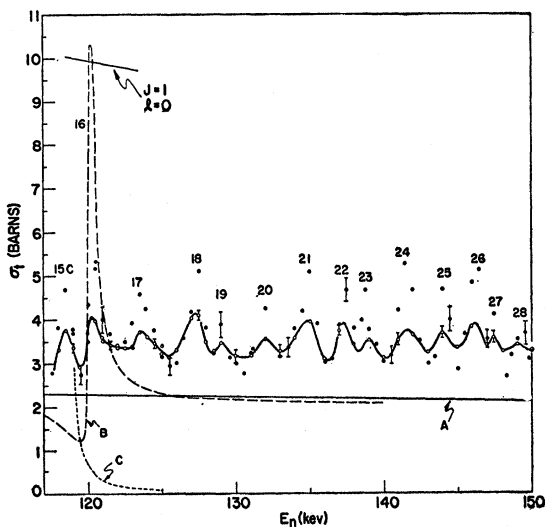


FIG. 11. Neutron total cross section of sodium from 120 to 150 keV. Open circles show the data obtained by flat detection; solid circles the data by self-detection. Curve A is a multiple-level plot of the *s*-wave levels that extend into this region. Curve B is a continuation (from Fig. 9) of the multiple-level plot of peaks Nos. 12, 14, and 16. Curve C is the high-energy wing of peak No. 15C.

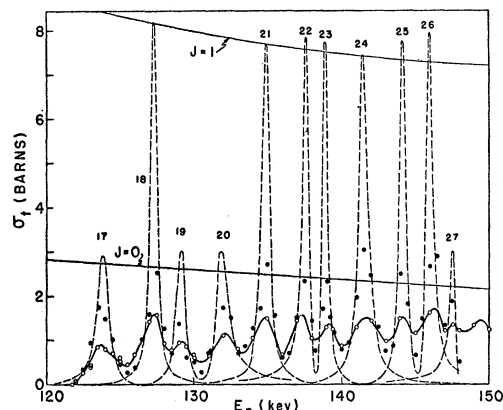


FIG. 12. Analyses of the levels of Na²⁴ from 120 to 150 keV. The points shown were obtained by subtracting curves A, B, C from the data in Fig. 11. The dashed curves show the theoretical plots obtained by use of the resonance parameters listed in Table I.

17, 19, and 20 was obtained by use of neutron widths of 0.90, 0.70, and 1.0 keV, respectively. This plot appears to agree with the data, particularly the self-detection data. A single-level plot for No. 18 is shown by a dashed curve in Fig. 12 for a width of 0.50 keV.

The observed heights of peaks Nos. 21 through 26, particularly by self-detection, indicate a value of $J>0$. Moreover, one would expect to resolve resonances of these apparent widths to higher peak values by use of smaller neutron energy spreads. The value of J for each resonance might then be taken to be 1. Therefore, if each resonance is attributable to a *p*-wave neutron interaction, a single multiple-level curve should account for this entire group of levels. However, the fact that peaks Nos. 21 and 24 appear to be somewhat wider than the remaining peaks may indicate that Nos. 21 and 24 are *p*-wave levels and that the widths of Nos. 22, 23, 25, and 26 may be sufficiently narrow for *d*-wave interactions. Accordingly, a multiple-level plot for Nos. 21 and 24 is shown in Fig. 12 for a *p*-wave interaction and a multiple-level plot for the remaining four peaks for a *d*-wave interaction. The various widths used to obtain these plots are listed in Table I. The depths of the minima between various pairs of resonances appear to further strengthen the assignments for the values of l . A discussion of peak No. 27 is reserved for inclusion with the next group of levels.

The data from 150 to 180 keV are displayed in Fig. 13 in which points obtained by flat detection are represented by open circles and those obtained by self-detection by solid circles. Curve A in Fig. 13 includes the potential-scattering cross section as well as the mutually interfering wings of all *s*-wave levels that extend into this region. When this curve is subtracted from the data, one has left only the resonance contributions of the levels in this region. These resonance contributions are shown by the solid curve in Fig. 14. The loci of the possible peak heights for $J=0$ and 1 are also shown in this figure.

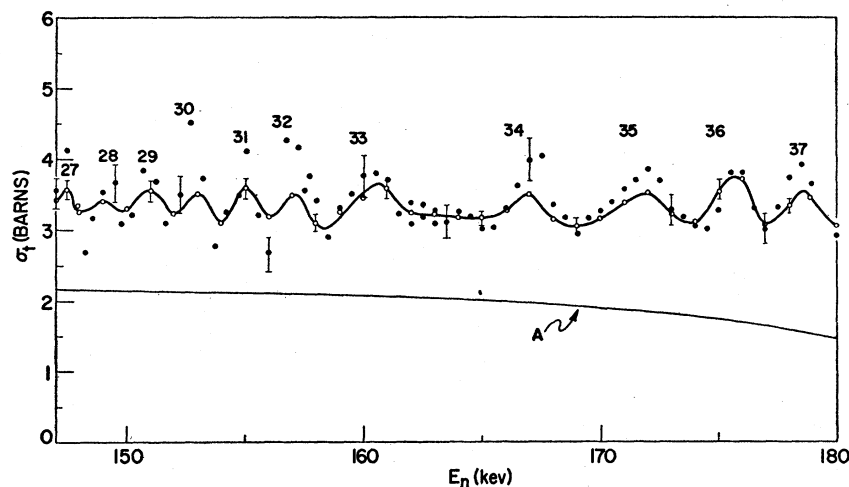


FIG. 13. Neutron total cross section of sodium from 147 to 180 keV. Open circles show the data obtained by flat detection; solid circles the data by self-detection. Curve *A* is a multiple-level plot of the *s*-wave levels that extend into this region.

In Fig. 14 one sees that these peaks divide into two groups according to level widths: (1) a group of relatively narrow levels comprising peaks Nos. 27 through 32, and (2) a second group of wider levels comprising peaks Nos. 33 through 38. The narrow peaks appear to divide into two subgroups according to peak heights. The data obtained by flat detection show peak heights well below possible values for $J=0$ for peaks Nos. 27 through 32. Taking into account the contribution of the high-energy wing of No. 26 to the peak of No. 27, the peak heights of Nos. 27 through 29 were practically unchanged by self-detection measurements. However, self-detection measurements increased the peak heights of Nos. 30 through 32 to values near those corresponding to the theoretical values for $J=0$. This increase in the observed peak heights over the amounts observed for Nos. 27 through 29 does not appear to be attributable

to differences in the widths because the widths of Nos. 30 through 32 appear to differ very little from the widths of Nos. 27 through 29 (for the same value of J). One, then, concludes that these differences in observed peak heights occurred because of differences in the true peak heights. Therefore, the value of J is taken to be 0 for Nos. 27 through 29 and 1 for Nos. 30 through 32. This, then, leads to two sets of mutually interfering levels. Deep minima would then be expected to occur between interfering levels. The observed minima appear to be sufficiently low between relevant pairs of levels to support these conclusions. The appropriate minima might be expected to be lower but in view of the small level spacings, one cannot resolve them to their true depths.

Suitable sets of parameters for the various levels represented by peaks Nos. 27 through 32 were deter-

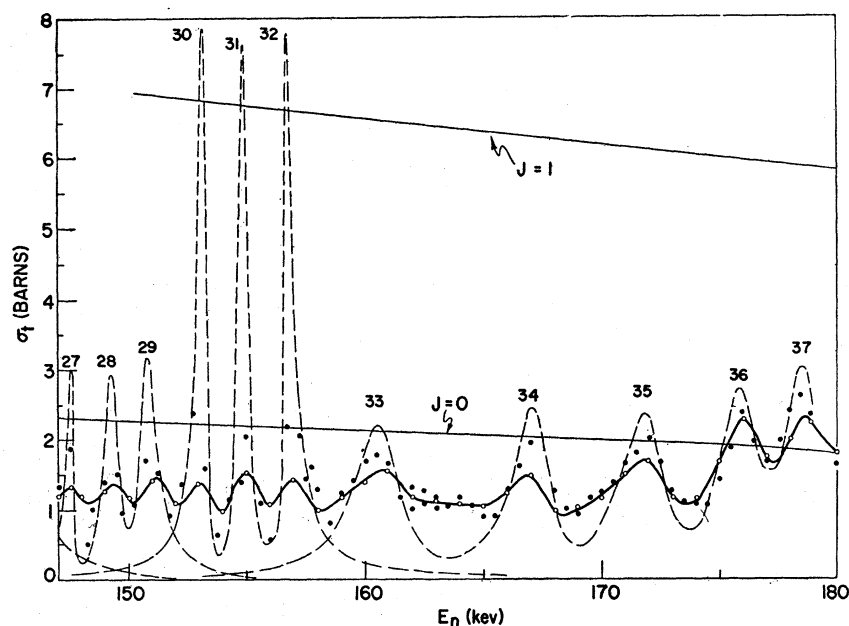


FIG. 14. Analyses of the levels of Na^{24} from 150 to 180 keV. The points shown were obtained by subtracting curve *A* from the data in Fig. 13. The dashed curves are the theoretical plots obtained by use of the resonance parameters listed in Table I.

mined by trial and error. A multiple-level plot is shown in Fig. 14 for Nos. 27 through 29 for $J=0$ ($l=1$), the widths used being listed in Table I. For Nos. 30 through 32, a second multiple-level plot is shown in Fig. 14 for $J=1$ and $l=2$ although this plot differs little from a similar plot for $l=1$. The widths used for this plot are also tabulated in Table I.

The peaks of the group of wider levels, Nos. 33 through 38, rise to observed heights close to or above the corresponding theoretical single-level peak heights for $J=0$, Nos. 37 and 38 being the highest. By a direct examination, one can see that the widths of these levels are close to 2 kev. Therefore, smaller neutron energy spreads would not be expected to resolve resonances of this apparent width to very much higher peak values. Hence, the value of J is taken to be 0 for each level in this group; and, because of their relatively large widths, the value of l is taken to be 1. For these assignments, mutual interference must occur. However, the depths of some of the minima between adjacent pairs of peaks appear to be insufficient to support these conclusions. On the other hand, the behavior of the cross section in the valleys between some of the pairs of adjacent peaks indicates the presence of some unresolved levels, particularly the valleys between peaks Nos. 33 and 34 and between Nos. 34 and 35. All of these peaks are then taken to be due to mutually interfering levels because no other assignment appears to be possible for the present data. By trial and error a best fit to the data was obtained. The multiple-level plot shown in Fig. 14 for these levels appears to agree with the data except for the two or three valleys between the peaks. In particular, the plot shows that, as observed, the mutual interference caused the peak heights of most of these levels to rise above the single-level heights.

E. Analysis of the Resonance Levels from 180 to 240 Kev

The large resonance observed by Stelson and Preston² just above 200 kev was found to be composed of two peaks, Nos. 42 and 43, shown in the upper curve of Fig. 15 in which points obtained by self-detection are represented by solid circles and those obtained by flat detection are represented by open circles. The splitting of this resonance into two peaks was observed twice by flat-detection measurements and later by self-detection. The combined configuration of these two peaks together with the overlapping wings of other nearby peaks indicates that No. 42 can be expected to be a relatively narrow p - or d -wave resonance. The high value of the cross section in the high-energy wing of Nos. 42 and 43 indicates an s -wave neutron interaction for No. 43. By trial and error it was found that the most reasonable fit for Nos. 42 and 43 could be obtained only by assuming No. 43 to be an s -wave resonance. Resonance No. 42 is then located at the

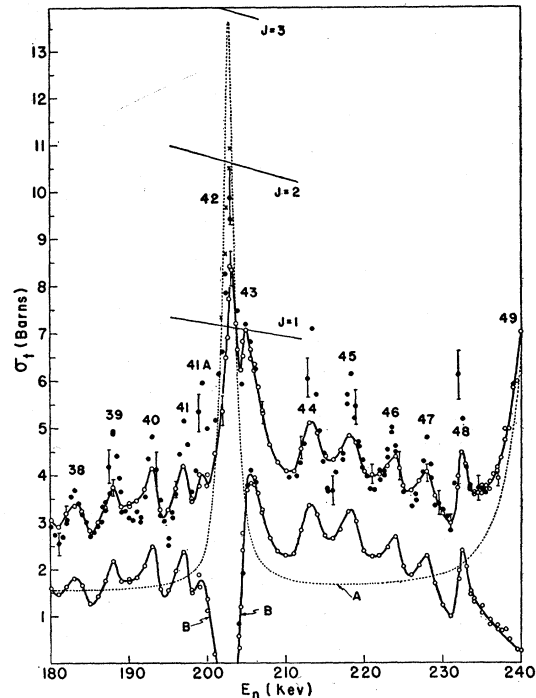


FIG. 15. Neutron total cross section (upper curve) of sodium from 180 to 240 kev. Open circles show data obtained by flat detection; solid circles data by self-detection. Curve A is a single-level plot for resonance No. 42 and includes the low-energy wing of No. 49 and the s -wave levels at higher energy. Curve B represents the difference between the data and curve A.

minimum of No. 43 and hence this minimum depresses the peak of No. 42 and also distorts the shape of the resonance. This distortion is clearly recognizable in Fig. 15. Repeated attempts to analyze this pair of resonances indicated that a best fit could be obtained by taking a value of $J=3$ for No. 42 with $\Gamma=1.8$ kev and $l=1$, although a value of $l=2$ can not be unambiguously ruled out. After the analyses were completed, the self-detection data near the peak of No. 42 were corrected for the depression caused by the minimum of No. 43. The corrected points are represented by crosses in the upper curve of Fig. 15. The highest corrected point is then very near the possible value for $J=2$ and rules out this value of J because a resonance of this width can not be expected to be resolved to a height so near its true value. Curve A in Fig. 15 includes the potential scattering, the combined single-level plots of No. 42 and No. 49 ($J=2$, $l=1$), the s -wave level No. 60, and the one at 542 kev. The wings of the s -wave levels, which were computed by the multiple-level dispersion formula [Eq. (2) of reference 7] show that the cross section is depressed throughout this region. By subtracting curve A from the data in Fig. 15, one obtains the two parts of curve B, which are then transferred to curve D of Fig. 16.

Because of its apparent asymmetrical shape and on the basis of the trial-and-error fit mentioned above,

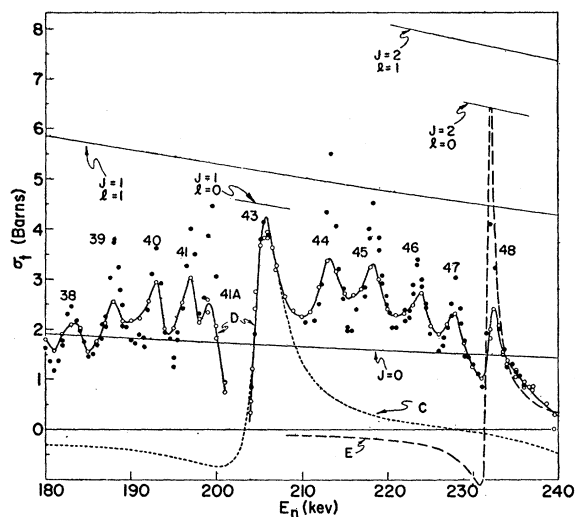


FIG. 16. Analyses of the levels of Na^{24} in the region from 180 to 240 keV. The points shown were obtained by subtracting curve *A* in Fig. 15 from the data. Curve *C* shows the multiple-level *s*-wave plot for Nos. 43 and 50. Curve *E* is a single-level plot for No. 48. Curve *D* from 180 to 200 keV has been corrected for the low-energy wings of resonance Nos. 43 and 48. The potential scattering is not included in any curve.

peak No. 43 is taken to be an *s*-wave resonance. The measured peak height is close to the theoretically possible height for $J=1$. Use of smaller neutron energy spreads would not be expected to resolve a resonance of this apparent width to any appreciably higher peak value. Therefore, it is considered well resolved and J has a value of 1. Curve *C* in Fig. 16 is a multiple-level plot of the *s*-wave levels Nos. 43 and 50, obtained by the parameters shown in Table I. These parameters were first obtained by trial and error and later confirmed by the computer GEORGE. The mutual interference of these two levels lowers the peak height of No. 43 below the single-level height and elevates the peak of No. 50 above its single-level height as shown by curve *C* in Fig. 16 and curve *E* in Fig. 19.

Because of the asymmetrical shape of peak No. 48, it is also taken to be an *s*-wave resonance. Its relatively narrow width prevents one from resolving its peak to a height sufficient to distinguish clearly between the two possible values of 1 and 2 for J . But the degree to which it is resolved, particularly by self-detection, shows a preference for a value of $J=2$. Moreover, one can account for the high-energy wing of this resonance more easily with a value of $J=2$. By trial and error it was found that a best fit occurs for a width of 0.90 keV. The single-level plot for the parameters $J=2$, $\Gamma=0.90$ keV, and $l=0$ is shown as curve *E* in Fig. 16. Curves *C* and *E* are then subtracted from the data to obtain the two parts of curve *F* in Fig. 17.

All of the peaks in the group comprising Nos. 44 to 47 inclusive (Fig. 17) appear to be symmetrical in shape so they are taken to be *p*- or *d*-wave resonances. The fairly deep minimum (revealed by self-detection)

between Nos. 44 and 45 is indicative of mutual interference between this pair of resonances and the same is true for Nos. 46 and 47. In view of these minima and the relative observed peak heights of these peaks, it is unlikely that all four peaks are attributable to the same value of J . Mutual interference is not indicated between Nos. 45 and 46 because they are far enough apart that a deep minimum would have been observed if present. The self-detection data indicate a value of $J=2$ for Nos. 44 and 45 and a value of $J=1$ for Nos. 46 and 47. The multiple-level plots shown in Fig. 17 were obtained by use of the parameters shown in Table I. These plots do not fully account for the various minima but are about as compatible with the various aspects of the data as one can expect. The deep minima shown by the multiple-level plots are not resolved to that extent experimentally because (a) the valleys as well as the peaks are too narrow to be fully resolved, and (b) overlapping wings of neighboring resonances elevate these minima above what is shown by the multiple-level plots, and (c) one cannot rule out the possibility of the presence of other narrow unresolved resonances.

In the region below 200 keV one finds no indications of *s*-wave resonances. The observed peak heights of Nos. 37 and 38 are higher than the theoretical value for $J=0$, but they are wide enough that their peaks would be expected to be considerably higher if J were to be 1. Moreover, the overlapping wings of other near-by levels elevate the peaks somewhat. This will elevate both peaks above their single-level heights. Further, the minimum between these peaks indicates mutual interference. Therefore, J is taken to be 0 for both resonances. Their widths indicate a value of $l=1$.

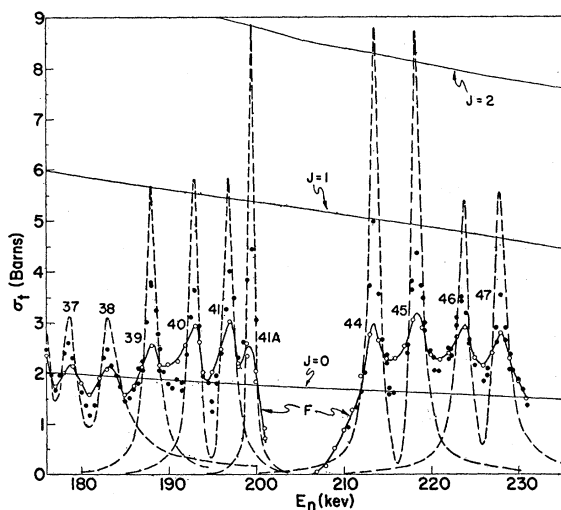


FIG. 17. A continuation of the analyses of the levels of Na^{24} from 176 to 230 keV. The potential scattering and the wings of *s*-wave levels were removed by the subtractions shown in Figs. 15 and 16. The dashed single- and multiple-level plots show the best fits for the resonances.

The multiple-level plot of Nos. 33 through 38 inclusive, obtained by a width of 1.9 kev for No. 37 and a width of 2.1 kev for No. 38, is shown in Fig. 17. This plot accounts very well for these two peaks. The value of J is taken to be 1 for peaks Nos. 39 to 41 inclusive because of their approximately equal peak heights. The apparent widths of these levels are too narrow to resolve to their true peak heights but sufficiently wide that one would have resolved the peaks to greater heights for a value of $J=2$. The minimum between Nos. 39 and 40 is not as deep as would be expected if there was mutual interference between resonances as well separated as these. On the other hand, mutual interference is assumed for peaks Nos. 40 and 41 because of the deep minimum between them. The self-detection data show that peak No. 41A is high and narrow with $J \geq 2$. Because of the nature of the data presented by the foregoing arguments, one must then necessarily assign a value of $l=1$ to No. 39 and $l=2$ to Nos. 40, 41, and 41A. The various plots obtained by the widths tabulated in Table I are shown in Fig. 17 and the sum of the plots appears to agree with the data except near the peaks.

F. Analysis of the Resonance Levels from 240 to 290 Kev

Two different measurements were made by flat detection over the region of peaks Nos. 49 and 50. The data are shown in the upper curve of Fig. 18, the points obtained in one run being represented by open circles and those of a second run by crosses. Resonance No. 49 is the predominant peak of this region and is the widest observed peak up to 500 kev. The wings are sufficiently

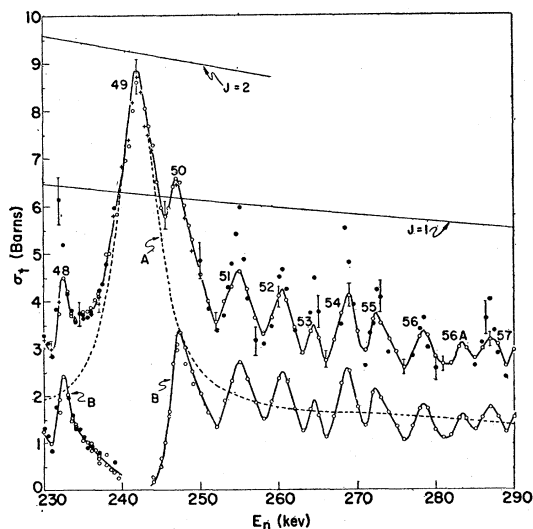


FIG. 18. Neutron total cross section (upper curve) of sodium from 230 to 290 kev. Open circles show data obtained by flat detection; solid circles data by self-detection. Curve A is a single-level plot for resonance No. 49. It includes the high-energy wing of No. 42 and the wings of s -wave levels at higher energy. Curve B represents the difference between the data and curve A.

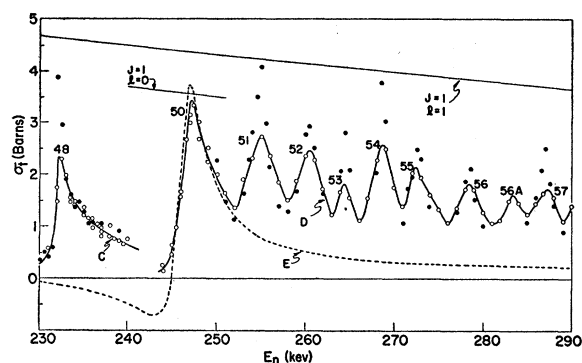


FIG. 19. Analyses of the levels of Na²⁴ in the region from 230 to 290 kev. The points shown were obtained by subtracting curve A from the data in Fig. 18. Curve E shows the multiple-level s -wave plot for resonance Nos. 43 and 50. Curve C has been corrected for the s -wave levels. The potential scattering is not included in any curve.

revealed to show that it is symmetrical in shape. Because of its large width, it is attributable to a p -wave neutron interaction. Also because of its large width, this resonance is undoubtedly well resolved and a value of $J=2$ appears to be certain. It is to be noted, however, that the low-energy wings of the s -wave level No. 60 and the one at 542 kev extend into this region and therefore depress the cross section everywhere in the region. Consequently the apparent peak height of resonance No. 49 should fall below the theoretical single-level value for $J=2$ even with perfect resolution. The curve designated by A in Fig. 18 is a single-level plot obtained by a width of $\Gamma=6.0$ kev and $l=1$. It includes a single-level calculation of the high-energy wing of No. 42 and also the low-energy wing of the s -wave level No. 60 and of the s -wave resonance at 542 kev. The low-energy wings of these s -wave levels were calculated from the multiple-level formula [Eq. (2) of reference 7]. The two parts of curve B in Fig. 18 were obtained by subtracting curve A from the data and were then transferred to Fig. 19 where they are labeled C and D. The analysis of resonance No. 48 is shown in Fig. 16.

With any reasonable widths of the resonances in the neighborhood of peak No. 50, subtracting their wings from the data yielded an asymmetric shape for the latter peak. In particular, the cross section in the high-energy wing of No. 50 is so high that an s -wave neutron interaction seems to provide the only possible means of accounting for it. Because of its width, this resonance is nearly completely resolved and the value of J is therefore taken to be 1. Curve E in Fig. 19 is a multiple-level plot of the s -wave resonances Nos. 43 and 50 and is a continuation of curve C in Fig. 16.

It is understandable that resonance No. 49, although 6 kev wide, is not resolved to its true single-level peak height for a value of $J=2$. This is attributable in part to the depression of the cross section in this region by the s -wave levels at higher energies and in part to the

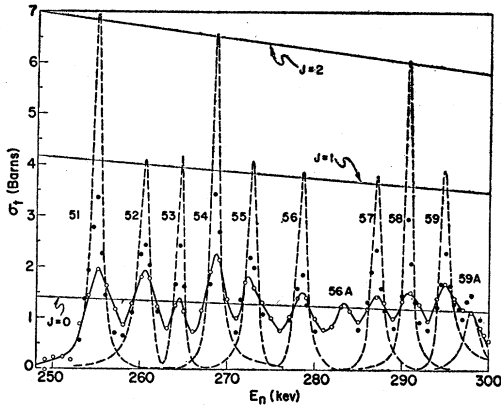


FIG. 20. A continuation of the analyses of the levels of Na^{24} from 250 to 300 keV. The potential scattering and wings of s -wave levels were removed by the subtractions shown in Figs. 18 and 19. The dashed single- and multiple-level plots show the best fits for the resonances.

fact that No. 49 is located very near the minimum of No. 50; but this extra depression caused by the minimum of No. 50 is mostly offset by the high-energy wing of the s -wave resonance No. 48 and the wings of other neighboring resonances. The calculated curve *A* in Fig. 18 includes the wing of the s -wave resonance No. 60 and of the one at 542 keV plus the high-energy wing of No. 42. The peak height of this curve can be seen to be a few tenths of a barn below the single-level height of No. 49. The close agreement of the calculated and observed peak heights of No. 49 then serves to indicate that the assumed value of the potential scattering cross section in this region is close to its true value. Resonance No. 50, having a width of 3 keV, might also be expected to be resolved very nearly to its true peak height but one sees in Fig. 19 that it is slightly below the multiple-level value. However, the multiple-level plot (curve *E* in Fig. 19) has not been corrected for the wings of neighboring resonances and therefore will be slightly higher than the observed peak height of No. 50.

By subtracting curve *E* in Fig. 19 from curve *D* one obtains the curve shown in Fig. 20. All of the peaks in this group (Nos. 51 through 59*A*) appear to be symmetrical in shape and are, therefore, attributable to p - and d -wave neutron interactions. The various single- and multiple-level plots shown in Fig. 20 were obtained by use of the parameters tabulated in Table I. These parameters were determined by trial and error. Peak No. 56*A* is a spurious reflection of the 2.95-keV resonance and arises because of the second group of low-energy neutrons in the beam.^{6,7} This peak is therefore not included among the levels of Na^{24} .

G. Analysis of the Resonance Levels from 290 to 350 KeV

The data for this region are shown by the upper curve in Fig. 21, where open circles represent points

obtained by flat detection and closed circles the points obtained by self-detection. Peak No. 60 is the predominant resonance in this region and clearly shows a pronounced minimum on its low-energy side. Its shape, although modified to some extent by neighboring peaks, is still distinctly asymmetrical and therefore is clearly attributable to an s -wave neutron interaction. The observed peak height is 5.5 barns (including the potential scattering) compared with theoretical single-level heights of 4.6 and 6.4 barns for $J=1$ and 2, respectively. Mutual interference with the s -wave resonance at 542 keV can be expected to reduce the peak height of No. 60 considerably because of the large width of the former. Therefore, the value of J is taken to be 2. By a direct examination, one can see that the width is approximately 2.5 keV. This was confirmed by a multiple-level plot for this resonance and the resonance at 542 keV. This plot is shown by curve *A* in Fig. 21, which also includes the contribution of the multiple-level plot of resonances Nos. 43 and 50 ($J=1, l=0$). By subtracting this curve from the data, one obtains curves *B* and *C*. Only curve *C* is then transferred to Fig. 22, curve *B* being included in Fig. 20. Peak No. 61 is attributable to $J=0$ and a single-level plot for $\Gamma_n=1.6$ keV and $l=2$ is shown by curve *D* in Fig. 21, this being about the best fit in view of the wings of neighboring levels.

No wide peaks or s -wave resonances are left in the region from 300 to 350 keV. The peak heights obtained by self-detection indicate that no peak has a value of J less than 1 and the relatively narrow widths indicate d - and f -wave neutron interactions. The observed peak height of No. 63 (self-detection) is near the possible value for $J=1$ and, for a resonance of this apparent width, one could expect by use of smaller neutron energy spreads to resolve this peak to a considerably

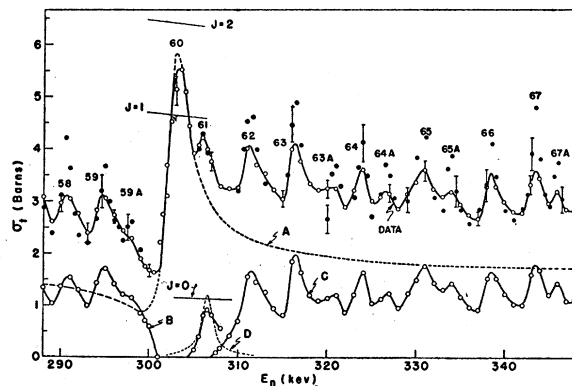


FIG. 21. Neutron total cross section (upper curve) from 288 to 348 keV. Open circles show data obtained by flat detection; solid circles data by self-detection. Above 325 keV the solid circles show self-detection data obtained for neutrons emitted in the direction of the proton beam. Curve *A* is the multiple-level s -wave plot of resonance No. 60 and the s -wave level at 542 keV. It also includes the multiple-level plot of resonances Nos. 43 and 50. Curves *B* and *C* were obtained by subtracting curve *A* from the data.

higher value which would be at least sufficiently high to rule out a value of $J=1$. Since the data show similar heights and widths for Nos. 63 and 67, the value of J is taken to be 2 for these two resonances. Peaks Nos. 62, 64, 65, and 66 are then attributable to $J=1$ because they are wider than Nos. 63 and 67 and their peaks are not as high (self-detection). The self-detection data on peak No. 63A also indicate a value of $J=1$ for this peak and it is then reasonable to conclude the same for Nos. 64A, 65A, and 67A. These latter peaks are so narrow that the value of l is 2, or preferably 3, for them. The appropriate single- and multiple-level plots are shown in Fig. 22. Single-level plots are shown for Nos. 63 and 67 for $l=3$ and a single-level plot is shown for Nos. 62, 64, 65, and 66 for $l=2$. A multiple-level plot is shown for Nos. 63A, 64A, 65A, and 67A ($l=3$). Although this multiple-level plot was obtained for $l=3$, it differs little from the one obtained for $l=2$. These plots were obtained by use of the parameters shown in Table I. The widths were determined by trial and error. The widths of these resonances are relatively narrow and it is entirely possible that one or more of them could be resolved to higher values of J by narrower neutron energy spreads. On the other hand, their widths are sufficiently wide that one can hardly expect to resolve them to heights much above those heights corresponding to the assigned values of the J 's. The corresponding reduced widths are so small that one expects that $l \geq 2$ for Nos. 61, 62, 65, and 66 and $l=3$ for all others.

5. STRENGTH FUNCTIONS

Values of the s - and p -wave strength functions have been obtained for the levels of Na²⁴ up to 350 kev. These strength functions are tentative and will be revised when the levels at higher energies can be included. The strength function⁷ is given by $(\gamma^2)_{n}/\bar{D}$, the ratio of the average reduced width to level spacing, where

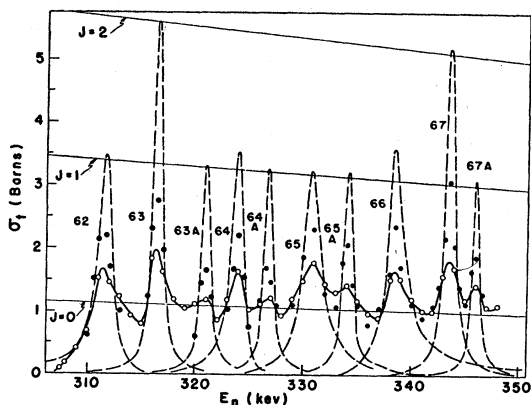


FIG. 22. Analyses of the levels of Na²⁴ from 306 to 350 kev. The potential scattering and wings of s -wave levels were removed by the subtraction shown in Fig. 20. The best fit is shown by the dashed curves obtained by the appropriate single- and multiple-level computations.

the reduced width $\gamma^2 = \Gamma_n / (2P_l)$ and D are averaged for a given value of l . Averaged over both values of J for s -wave levels ($l=0$), the strength function is 0.06; and averaged over all observed values of J for p -wave levels ($l=1$) it is 0.65, which is approximately ten times as large as for s -wave levels. These results are in accord with the complex square-well model of Feshbach, Porter, and Weisskopf¹⁷ who, for a nuclear well depth of 40 Mev, predict a maximum in the strength function for the p -wave levels in the region of $A=25$ and a low value for s -wave levels. The sum rule of Lane, Thomas, and Wigner¹⁸ suggests that the sum of the reduced widths of a given group of resonances in an energy interval comparable with the spacings of giant resonances for a given l should not exceed $\hbar^2 / (\mu R^2)$. For the p -wave levels in the present measurements, this sum is about 0.37 of the Wigner limit and indicates that this interval of energy is near the maximum for the strength function for $l=1$. The strength functions for the d - and f -wave levels are much too high in comparison with the p -wave strength functions. This could in part be the result of having assigned too many levels to $l=2$ and 3. On the other hand, because of nuclear shell effects, it is conceivable that the expressions for the penetrability factors P_2 and P_3 are incorrect and could cause large errors in the reduced widths and hence in the strength functions. A third possibility is that the reduced width γ^2 may depend on the value of l .

6. DISCUSSION

The results show an unexpectedly large number of levels, many of which have relatively narrow widths. The observed range in widths was from 0.2 to 6 kev, compared with a range⁷ from 1 to 7 kev for Al²⁸. Because of the profusion of narrow widths, many of the levels were studied intensively in order to determine their J values. Most of the levels were also studied by self-detection, which aided materially in the analyses. In the region between 60 and 180 kev, many narrow levels were observed. These levels are too narrow to be resolved sufficiently by present techniques to determine their parameters accurately. However, one can determine minimum values for J and hence maximum values of the widths. Undoubtedly the parameters of these levels will then produce some irregularities in the distribution of the angular momenta, level spacings, and neutron widths. The results of the most recent measurements, which are shown in the various figures, show the highest peak values obtained and the lowest minima between peaks. The neutron energy spreads used ranged between 300 and 400 ev according to the rise-curve method^{6,7} but were generally about the smallest usable, namely, about 300 ev. At the higher

¹⁷ H. Feshbach, C. E. Porter, and V. F. Weisskopf, Phys. Rev. **96**, 448 (1954).

¹⁸ A. M. Lane, R. G. Thomas, and E. P. Wigner, Phys. Rev. **98**, 693 (1955).

energies the energy spread is expected to be larger; but no good estimate of the energy spread can be made because no really well isolated level of sufficiently narrow width has been found. However, peak No. 48 in Fig. 16 does provide a rough estimate. Its width appears to be about 0.9 kev and, since it is apparently an *s*-wave level, the value of J cannot exceed 2. The degree to which it is resolved, then, indicates that the neutron energy spread around 250 kev is not more than 500–600 ev. The degree to which the various levels of different widths are resolved appears to agree with measurements that have been made on other elements for which the level spacings are greater.

The levels previously observed² above 200 kev were all found to be composed of two or more levels. This accounts largely for the difficulties encountered by Lane and Monahan¹⁹ in attempting to analyze their data on the angular distribution measurements in this region.

Values of the strength functions obtained for the *s*- and *p*-wave levels are comparable with those⁷ obtained for Al²⁸ and are in accord with the predictions of theory.¹⁷ Very high values of the strength functions for *d*- and *f*-wave levels could be attributed to assigning too many levels to *d*- and *f*-wave interactions. However, only a relatively small number of levels were so assigned and undoubtedly a number of the levels in this energy interval are expected to belong to values of $l=2$ and 3. In this work and the work on aluminum, it appears that either the theoretical values for P_l or γ_l^2 for $l>1$ are

¹⁹ R. O. Lane and J. E. Monahan, Argonne National Laboratory Report ANL-5554, 1956 (unpublished), p. 22; and private communication.

far too small. This produces unusually large reduced widths and hence large strength functions.

Because of the arguments given in Sec. 4A, the potential scattering was taken to be given by the expression

$$\sigma_p = \sum_l (2l+1)4\pi\lambda^2 \sin^2\delta_l.$$

In view of the results obtained by the analyses, this value of the potential scattering cross section appears to be about right.

Initial measurements have been made up to 500 kev, but because of the density of levels, it is planned to reinvestigate the region from 350 to 500 kev by self-detection and to extend the measurements up to higher energies. These measurements will be made by neutrons emitted in the direction of the proton beam and will be given in a subsequent paper. It will include plots of the distributions of the angular momenta, level spacings, and neutron widths for all of the levels of Na²⁴.

ACKNOWLEDGMENTS

I wish to express my appreciation to Dr. F. E. Throw for his comments and suggestions with the manuscript, to Jack Wallace for his aid in operating the Van de Graaff generator, to the Van de Graaff crew consisting of Walter Ray, Jr., William Evans, Robert Kickert, John Bicek, Robert Petersen, and Joseph Ragusa, and also to Leo Lacknowicz of the Central Shops for his work in preparing the sodium metal samples. I also wish to thank the Applied Mathematics Division for much of the detailed computations which were necessary in fitting the level parameters to the data.